UDC 621.315.592

Kulikov S.S., Brytavskyi Ye.V., Borshchak V.A.,
Zatovskaya N.P., Kutalova M.I., Karakis Y.N.

Odesa I. I. Mechnikov National University, 2, Dvoryanskaya str.
phone: 723-34-61 e-mail:photoelectronics @onu.edu.ua

THE STUDY OF HOMOGENEOUS AND HETEROGENEOUS SENSITIZED CRYSTALS OF CADMIUM SULFIDE. PART V. HETEROGENEOUS DOPPING

.

A technology for processing semiconductor crystals in a corona discharge has been developed. It w2as found that as a result of this exposure, the samples acquire alternating spectral sensitivity. The observed phenomena are explained by the appearance of a two-pitched potential barrier in the near-surface region of the element, the unusual properties of which may allow the creation of a new type of device.

Introduction

This publication is a continuation of the reviews [1-4]. In order to preserve the generality of the work, the numbering of sections is selected general. Numbers of formulas and figures are presented by sections. References to the literature in each review are given individually.

Cadmium sulfide crystals are used in our research as a convenient model material. The results obtained on them and the constructed models also apply to other semiconductor substances.

In the previous parts of the review, it is considered how the photovoltaic properties of a semiconductor changes, in which, under the influence of external factors (light, electric field, temperature), the redistribution of a sensitive impurity occurs. Samples in which the conductivity is controlled by the Bube-Rose model are selected as systems that are particularly sensitive to these influences. That is, crystals initially already contain R – and S-centers.

It is of interest to investigate how the properties of the elements will change if the alloying additive itself is an external factor. That is, a change in the photoelectric properties of initially uniformly alloyed samples, in the contact layers of which, from the surface, an alloying impurity appears.

It should be noted that the heterogeneous distribution of the impurity in this case is a typical situation that one has to face in practice.

It is known that the properties of semiconductor crystals can vary widely depending on the quantity and quality of the defects formed. This should also affect the contacting part of the semiconductor sample.

In this paper, we consider the problem of the behavior of ohmic contact to a semiconductor in the initial state when unevenly distributed charged electron traps appear in its spatial charge region. Despite the urgency of this problem, it is practically not covered in the literature.

The introduction of trap centers into the contact layer of the crystal can radically change the energy structure of this area. In particular, in the case of electronic traps, the formation of a locking barrier is possible. At the same time, the conditions of current transfer change significantly and specific effects occur that are close in nature to negative photoconductivity.

To analyze this situation, it is necessary to derive dependencies describing the type of barrier that occurs in the conduction band, both in the dark and in the light. As well as determining the relationship of the parameters of this barrier – its width, height, coordinates of the maximum, the steepness of the walls - from the properties of the traps – their energy

depth, initial concentration and distribution over the depth of the sample.

The goal of this work is to show that unevenly distributed charged electron traps are able to form a locking barrier in the area of the spatial charge of the ohmic contact. Its parameters are uniquely related to the parameters of traps and, therefore, are controlled technologically. At the same time, due to the barrier that has arisen, the sensor based on a semiconductor crystal acquires new properties, including anomalous ones.

Changes in photoconductivity caused by the treatment of single-crystal samples of cadmium chalcogenides in a gas discharge were investigated by the authors [5-7]. The technology of such processing is as follows. The element was placed in a vacuum ” 10^{-2} 10^{-3} mmHg. between the electrodes, to which a voltage of the order of several kilovolts was applied. Variable fields of industrial frequency were used. In the resulting discharge streamer, charged particles bombard the sample surface. It has been established that gas discharge treatment of the surface of cadmium chalcogenide crystals leads to the creation of a large concentration of electron traps in the near-surface layer.

In the case of crystal excitation by strongly absorbed light, nonequilibrium carriers are created in a thin near-surface layer. At the same time, it should be borne in mind that the treatment of a single crystal with a gas discharge, it is in this layer that causes an increase in the concentration of traps. Therefore, the change in photoconductivity in this case depends on the ratio of the depth of penetration of exciting light into the sample and the depth of propagation of the trap centers. The most favorable condition for changing the photoconductivity can be considered the coincidence of the depth of light penetration with the depth of propagation of traps.

In a pure semiconductor for ohmic contact, the energy distribution changes according to the logarithmic law

$$E = 2kT \ln\left(1 + \frac{x}{a}\right) \tag{8.1}$$

where, a there is some characteristic length.

The distribution of the electron concentration in this case is expressed by the ratio

$$n = n_k \exp\frac{E}{2kT} = n_k \left(\frac{a}{a+x}\right)^2 \tag{8.2}$$

Thus, the semiconductor layers bordering to the metal electrodes, the thickness of which ~ a, they can be "filled" with charge carriers. At the same time, the concentration of carriers near the contacts n_k, as formula (8.1) shows, it does not depend on their concentration in the depth of the semiconductor, which may be small (insulator). Therefore, the electrical conductivity of such a contact can be high, even if the specific electrical conductivity of the semiconductor (in the absence of contact) is negligible, for example, in the case of a wide-band CdS.

8.1. The effect of traps on the barrier structure

If the contact is formed for a high-resistance semiconductor, then due to the significant difference in conductivities, almost the entire area of the spatial charge (ASC) is located in its contact layer.

Let electronic traps be introduced into such a semiconductor N_t, the concentration of which decreases from the surface deep into the volume according to the law

$$N_t = N_{t0} e^{-\frac{x}{l_0}}, \tag{8.3}$$

where N_{t0} – this is their concentration on a geometric surface, and l_0 – a characteristic length showing at what distance the number of traps decreases in e times.

The activation energy of these traps (E_c–E_t). Then, directly at the contact (area I fig. 8.1), the traps end up under the Fermi level. Such traps are filled with electrons regardless of the concentration of free charge. On the surface itself, their distance from the Fermi energy and, consequently, filling, will be maximal. Therefore, at the point x=0 the appearance of such traps will not change the concentration of free electrons and the distribution of energy. They are still described by formulas (8.1) and (8.2).

As can be seen from Figure 8.1, the greater the depth of the traps (E_c–E_t), the wider the

electron-enriched region I, since up to large x coordinates the traps are located below the Fermi level or in the Fermi level region.

At the same time, as will be shown in more detail below, the greater the initial concentration of traps N_{t0}, the steeper the dependence $\frac{dE}{dx}$ goes up . Both of these factors, acting together, should ensure a greater height of the barrier formed.

On the contrary, in the depth of the volume at $x > L_1$ the appearance of electronic traps will change the conditions significantly. The traps are partially filled and are able to capture an additional charge. In this case, the concentration of the free charge, initially constituting n_0 (curve 1 Figure 8.1), it should decrease, which is accompanied by an increase in the distance from the bottom of the conduction band to the Fermi level.

Consider the far edge of the impurity propagation front N_t (area III of Figure 8.1). The concentration of traps in the area $x = L_1$ it is small, so in general it remains electroneutral. Part of the free charge goes to the traps. The equation of electroneutrality in this case looks like this:

$$N_d^+ = n_0 e^{-\frac{E(x)}{kT}} + N_{t0} e^{-\frac{x}{\ell_0}} . \qquad (8.4)$$

Taking into account that numerically the concentration of ionized donors N_d^+ equal to n_0 and using the exponential expansion in a series, from (8.4) we obtain

$$n_0 \frac{E(x)}{kT} = N_{t0} e^{-\frac{x}{\ell_0}} .$$

Where from

$$E_3(x)\Big|_{x \to L_2} = \frac{N_{t0}}{n_0} kT e^{-\frac{x}{\ell_0}} . \qquad (8.5)$$

As the x coordinate decreases towards the surface, the energy value of the edge of the conduction band increases, although slightly. If the whole free charge n_0 will switch to traps, then $(E–E_c) \sim kT$ (on the border of regions II and III).

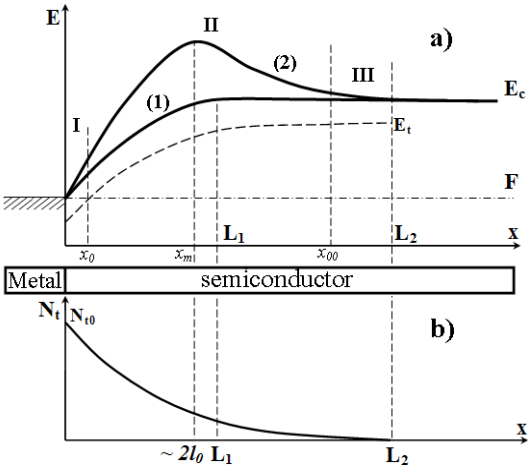

Fig. 8.1. (a) – the structure of the ASC ohmic contact to a high-resistance semiconductor: (1) - initial state; (2) - after the introduction of traps; (b) - distribution of the concentration of electronic traps by depth

The processes considered at the edges of the ASC are sufficient to predict changes in the energy distribution. If there is an energy curve in the depth of the volume $E_c(x)$ rushes upwards, and at the very contact with the metal comes to the same point where it was without taking into account traps, then in general the ASC profile should have the form of a bell-shaped maximum (curve 2 Fig. 8.1a). Moreover, its width is controlled only by the penetration depth of electronic traps, determined by the technological factors of crystal processing.

8.2. Energy distribution in the contact layers of a crystal with electron traps

The barrier profile in area I of Figure 8.1 a can be determined using the Poisson equation

$$\frac{d^2E_1}{dx^2} = \frac{4\pi e^2}{\varepsilon}\rho(x) = \frac{4\pi e^2}{\varepsilon}\left[N_d^+ - N_t(x) - n(x)\right], \qquad (8.6)$$

where E – energy, and $N_d^+ = n_0 << n_k$. Using expressions (8.2) and (8.3) formula (8.6) acquires the form:

$$\frac{d^2E_1}{dx^2} = \frac{4\pi e^2}{\varepsilon}\left[-N_{t0}e^{-\frac{x}{\ell_0}} - n_k\left(\frac{a}{a+x}\right)^2\right]. \qquad (8.7)$$

Note that negative values of the second derivative indicate the convexity of the function E_1 within area I. After integration

$$E_1(x)=\frac{4\pi e^2}{\varepsilon}\left[-\ell_0^{\,2}N_{t0}e^{-\frac{x}{\ell_0}}+n_k a^2\ln|a+x|+C_1x+C_2\right] \tag{8.8}$$

values of constants C_1 and C_2 can be determined from a comparison with the distribution (8.1) for a pure semiconductor.

When used for metal contacts with possibly small output operation, the value of the jump at the boundary $\Delta E\ (0) \to 0$. In this case, when x=0 $(E_c–F) = 0$ and $n_k \approx N_c = 10^{19}sm^{-3}$. According to [8], the value of the cadmium concentration on the surface $\sim 10^{21}sm^{-3}$. Taking this amount as 0.1-1% of the total value, we get that on the surface it is true $N_{t0} \le n_k$.

Taking into account also the calculations given in clause 8.1, regarding the filling of traps without changing the concentration of free charge, it will be fair:

$$\frac{dE}{dx}\Big|_{x=0}=\frac{dE_1}{dx}\Big|_{x=0}$$

or from (8.7) and (8.1):

$$\frac{2kT}{a+x}=\frac{4\pi e^2}{\varepsilon}\left[\ell_0 N_{t0}e^{-\frac{x}{\ell_0}}+\frac{n_k a^2}{a+x}+C_1\right],$$

when x = 0:

$$C_1=\frac{2kT}{a}\frac{\varepsilon}{4\pi e^2}-\ell_0 N_{t0}-n_k a \quad . \tag{8.9}$$

The value of the constant C_2 in (8.8) can be found from the condition $E_1\ (0) = 0$. It follows from it

$$C_2=\ell_0^{\,2}N_{t0}-n_k a^2\ln a \quad . \tag{8.10}$$

Finally (8.8), taking into account (8.9) and (8.10), takes the form:

$$E_1(x)=\frac{4\pi e^2}{\varepsilon}\left[\ell_0^{\,2}N_{t0}\left(1-e^{-\frac{x}{\ell_0}}\right)+n_k a^2\ln\frac{a+x}{a}+\left(\frac{2kT}{a}\frac{\varepsilon}{4\pi e^2}-\ell_0 N_{t0}-n_k a\right)x\right] \tag{8.11}$$

The resulting expression is too cumbersome for further analysis. Therefore, we assume that the value of l_0 in the distribution of traps is large enough, and the stitching point with the function $E_2\ (x)$ (i.e., the width of the area I) lies at a coordinate smaller than the radius of the shielding *a.* Then putting the exponent and the logarithm in a row, from (8.11) the expression is obtained:

$$E_1(x)=\frac{2kT}{a}x \quad , \tag{8.12}$$

which, as expected, is not affected by trap parameters l_0 and N_{t0}. In the near-surface layer, the energy distribution in the barrier is represented by an almost straight line with a slope *2kT/a.* At the same time, the graph $E_1(x)$ lies above the curve 1fig. 8.1a. That is, from the very beginning, with the growth of the coordinate, the concentration of the free charge drops faster than the concentration of traps.

8.3. Barrier structure in the depleted layer

In the central part of the barrier (region II of Figure 8.1), there is practically no free charge and the concentration of electrons on the traps significantly exceeds the number of ionized donors, since for these distances x the number of traps themselves is still quite large. Then $n_t(x) >> N_d^+$; $n(x)$. In this case, the charge density:

$$\rho(x)=-en_t(x)=-eN_t(x)f(x) \quad ,$$

where $f(x)$ - Fermi-Dirac probability for filling traps:

$$f(x)=e^{-\frac{(Ec-E_t)-(Ec-F)}{kT}}=e^{-\frac{Ec-E_t}{kT}}\cdot e^{-\frac{Ec-F}{kT}} \quad .$$

In this expression, the first exponent associated with the activation energy of the traps does not change with the coordinate, and the exponent of the second exponent depends on *x*.

Finally, the Poisson equation has the form

$$\frac{d^2E_2(x)}{dx^2}=-Ae^{-\frac{x}{\ell_0}}e^{\frac{E_2}{kT}} \quad , \tag{8.13}$$

where

$$A=\frac{4\pi e^2}{\varepsilon}N_{t0}e^{\frac{E_c-E_t}{kT}} \quad . \tag{8.14}$$

It can be seen that in this whole area the second derivative is negative. The curve is concave. Using substitution

$$Z = -\left(\frac{x}{\ell_0} + \frac{E_2}{kT}\right), \quad (8.15)$$

we have

$$\frac{d^2 z}{d\,x^2} = \frac{A}{kT} e^Z \quad . \quad (8.16)$$

Or

$$\frac{1}{2} d\left(\frac{dz}{dx}\right)^2 = \frac{A}{kT} e^Z dz \quad .$$

From where after integration

$$\left(\frac{dz}{dx}\right)^2 = 2\frac{A}{kT} e^Z + C_1 \quad . \quad (8.17)$$

The value of C_1 can be obtained at the maximum position, where $\frac{dE}{dx} = 0$. When

$$C_1 = \left(\frac{1}{\ell_0}\right)^2 - 2\frac{A}{kT} e^{-\frac{x_{\max}}{\ell_0}} \cdot e^{-\frac{E_{\max}}{kT}} \quad . \quad (8.18)$$

On the ascending curve, where $x<x_{max}$ *and* $E<E_{max}$ rightfully (see 8.15)

$$C_1 << 2\frac{A}{kT} e^Z \quad .$$

For sufficiently sharp barriers on the descending part of the magnitude x and x_{max} of the same order, and $E<E_{max}$. Therefore, this condition remains true here. In general, the formula (8.17) takes the form:

$$\left(\frac{dz}{dx}\right)^2 = 2\frac{A}{kT} e^Z \quad .$$

Where

$$\frac{dz}{dx} = \pm\sqrt{\frac{2A}{kT}} e^{\frac{Z}{2}} \quad . \quad (8.19)$$

In accordance with (8.11), the derivative is negative on the ascending part of the curve. On the falling part for everyone $\frac{dE}{dx} < \frac{kT}{\ell_0}$ (that is, a slow decline), this also remains in force. Then the "–" sign should be left in (8.19). As a result, after integration, it is determined

$$-2e^{-\frac{Z}{2}} = -\sqrt{\frac{2A}{kT}} x - C_2 \quad . \quad (8.20)$$

Substituting (8.15) into (8.20) and simplifying the expression, we get

$$E_2(x) = -kT\frac{x}{\ell_0} + 2kT \ln\left(\sqrt{\frac{A}{2kT}} x + C_2\right) . \quad (8.21)$$

8.4. Detailing of the energy distribution function explicit form

From the equality of derivatives at the crosslinking point x_0 is:

$$\frac{2kT}{a} = -\frac{kT}{\ell_0} + \frac{2kT\sqrt{\frac{A}{2kT}}}{x_0\sqrt{\frac{A}{2kT}} + C_2} \quad ,$$

therefore for the big ones l_0, where $\frac{1}{2\ell_0} << \frac{1}{a}$, we get

$$x_0\sqrt{\frac{A}{2kT}} + C_2 = a\sqrt{\frac{A}{2kT}} \quad (8.22)$$

Then the value

$$x_0 = a - \frac{C_2}{\sqrt{\frac{A}{2kT}}} \quad . \quad (8.23)$$

After substituting it into the expression $E_1(x_0) = E_2(x_0)$ we find:

$$\frac{2kT}{a}\left(a - \frac{C_2}{\sqrt{\frac{A}{2kT}}}\right) = -\frac{kT}{\ell_0}\left(a - \frac{C_2}{\sqrt{\frac{A}{2kT}}}\right) + 2kT\ln\left(a\sqrt{\frac{A}{2kT}}\right) \quad . \quad (8.24)$$

In the second term on the right in (8.24), the dependence (8.22) is taken into account. Re-

ducing by $2kT$ and giving similar ones, we get for $2\ell_0 >> a$

$$\left[1-\ln\left(a\sqrt{\frac{A}{2kT}}\right)\right]\cdot a\cdot\sqrt{\frac{A}{2kT}}=C_2 \quad (8.25)$$

If the increasing part of the barrier is sharp enough, then the value x_0 in (8.23) is not great compared to a. In this case, from equation (8.23) and (8.25) follows

$$\ln\left(a\sqrt{\frac{A}{2kT}}\right)<<1$$

and finally

$$C_2=a\sqrt{\frac{A}{2kT}},$$

$$E_2(x)=-\frac{kT}{\ell_0}x+2kT\ln\left[\sqrt{\frac{A}{2kT}}(x+a)\right]. \quad (8.26)$$

As can be seen from (8.26) at the maximum when

$$\frac{dE_2}{dx}=-\frac{kT}{\ell_0}+\frac{2kT}{x_m+a}=0,$$

meaning $x_m=2\ell_0-a\approx 2\ell_0$. (8.27)

The width of the increasing part of the barrier and, consequently, the field strength here is controlled by the parameters of the trap distribution $2l_0$. Substituting (8.27) into (8.26) determines the value of the function E_2 at the maximum:

$$E_{2\max}\cong -2kT+2kT\ln\sqrt{\frac{A}{2kT}}(2\ell_0). \quad (8.28)$$

More than $2l_0$, the higher the barrier.

Dependence on the initial concentration of traps N_{t0} and their activation energies (E_c–E_t) is set by the value

$$A=\frac{4\pi e^2}{\varepsilon}N_{t0}e^{\frac{E_c-E_t}{kT}}.$$

It follows from (8.28) that with an increase in these parameters, the height of the barrier also increases linearly proportionally $(E_c - E_t)$ and logarithmically proportional N_{t0}.

The total width of the ASC can be determined when $E_2(x)$=0:

$$\frac{L_2}{2\ell_0}=\ln\left(\sqrt{\frac{A}{2kT}}L_2\right). \quad (8.29)$$

It is taken into account here that, according to the conditions of the problem, the traps diffuse further L_1 and already at the maximum coordinate $x_{max}>a$. Equation (8.29) does not explicitly allow to obtain the dependence $L_2(l_0, A)$, but it allows us to identify the trends of this dependence using methods borrowed from number theory.

Imagine (8.29) as

$$\frac{L_2}{2\ell_0}-\ln L_2=\ln\sqrt{\frac{A}{2kT}}. \quad (8.30)$$

Let the type of traps not change (i.e. “A" is fixed), but due to technological techniques it increases l_0. In this case, since the right part does not change, and the denominator of the first term increases, the value L_2 it should increase, although not proportionally. If only L_2 it did not change, the left part (8.30) also decreased. This follows from

$$\frac{d\left(\frac{L_2}{2\ell_0}-\ln L_2\right)}{dL_2}=\frac{1}{2\ell_0}\downarrow-\frac{1}{L_2}\uparrow<0.$$

On the contrary, let l_0=const, and the value of "A" increases. Then the left part at (8.30) should increase. Since the logarithmic function $y=\frac{L_2}{2\ell_0}$, y=lnL_2 changes slower than linear, generally L_2 increases. With the increasing concentration of traps on the surface N_{t0} and their activation energies (E_c–E_t) the width of the ASC increases.

Note at the same time that for such a conclusion, it is important to simultaneously increase both parameters. In principle, a situation is possible when deeper traps

[$exp\left(\frac{E_c-E_t}{kT}\right)$ more] on a geometric surface is not enough (N_{t0} less). Since the value of N_{t0} managed technologically, this competition can be avoided.

8.5. Energy profile of the barrier in the semiconductor volume

After stitching at the point x_0 type of function $E_2(x)$ the depth of the volume also turned out to be related to the state of the surface (see 8.6). The standard procedure for stitching in depth volume functions $E_2(x)$ and $E(x)$ leads to an overly complex system of equations that can be solved only by numerical methods.

Therefore, an artificial technique was used [9]. Function value $\frac{dE_2}{dx}$ at the maximum when $x=x_m$ is equal

$$\frac{dE_2(x_m)}{dx} = -\frac{kT}{\ell_0} + \frac{2kT\sqrt{\frac{A}{2kT}}}{\sqrt{\frac{A}{2kT}}x_m + C_2} = 0 .$$

when $\sqrt{\frac{A}{2kT}}x_m + C_2 = 2\ell_0\sqrt{\frac{A}{2kT}}$

and $C_2 = \sqrt{\frac{A}{2kT}}(2\ell_0 - x_m)$.

This after substituting in $E_2(x)$ gives

$$E_2(x) = -\frac{kT}{\ell_0}x + 2kT\ln\left[\sqrt{\frac{A}{2kT}}(x + 2\ell_0 - x_m)\right]$$

and at the maximum ($x=x_m$)

$$E_{2\max} = -\frac{kT}{\ell_0}x_m + 2kT\ln\left(\frac{A}{2kT}4\ell_0^{\,2}\right). \quad (8.31)$$

It can be seen that the closer to the interface the barrier is formed (x_m decreasing), the higher it is. With the increasing concentration of traps N_{t0} and their depths ($E_c - E_t$) (i.e. "A" increases) the barrier is also increasing. This is the same as the one received earlier.

At the stitching point of the barrier function $E_2(x)$ with a function in the quasi-neutral domain, the value $E \approx kT$. Therefore, we can assume that x_m determines the overall width of the ASC: $x_m=L_2$. Obtain:

$$2\ln\left[\sqrt{\frac{A}{2kT}}(L_2 + 2\ell_0 - x_m)\right] = \frac{L_2}{\ell_0} + 1 ,$$

when $L_2>>l_0$ and therefore, $\frac{L_2}{\ell_0} >> 1$.

When $L_2 + 2\ell_0 - x_m = \frac{e^{\frac{L_2}{2\ell_0}}}{\sqrt{\frac{A}{kT}}}$,

or

$$L_2 \approx 2\ell_0\ln\left(2\ell_0\sqrt{\tfrac{A}{2kT}}\right). \quad (8.32)$$

The width of the spatial charge area increases with growth $2l_0$, which also coincides with what was received earlier.

8.6. Sample doping technology

The article [6] describes a method for creating electronic traps on the surface of a semiconductor by treating it with a gas discharge. The advantages of this technique are associated with the presence of an electric field during technological operations. By varying the magnitude and direction of this field, it is possible to control the process of introducing defects and the profile of their distribution.

At [10] indicates a significant migration of impurity ions in wide-band semiconductors in fields of the order 10^5 V/m.

In addition to creating electronic traps and a controlled process of their introduction into the volume of a semiconductor sensor, the proposed corona discharge processing method promotes the formation of donors on the sample surface [7]. The same electric field that promotes the outflow of electronic traps accumulates donors at the surface, increasing the conductivity in the subsurface layers. In this case, it becomes possible to process crystals with already applied contacts and in the same cycle to make measurements without the presence of air in the chamber.

The sample under study was a rectangular plate of monocrystalline cadmium sulfide with a thickness of 1.5 mm and a frontal surface area of about one square centimeter. The crystal was placed in a vacuum chamber, where a vacuum of the order of 10^{-2}–10^{-3} mmHg was created.

A stable symmetrical discharge (Fig. 8.2.b) was created [11] when the end of the cathode was given a conical shape. With an insufficient degree of discharge in the chamber, the discharge turned into an avalanche and was laced, and in the working area of high voltages, the moment of lacing practically did not depend on the field. All the results given below were obtained after processing in the glow discharge mode.

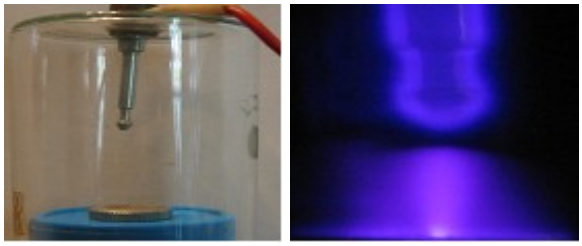

(A) (B)

Fig. 8.2. The design of the spark gap (A) and the processing of samples in vacuum in a gas discharge (B)

The best results were obtained with a gap of 8-12 mm. We attribute this to the fact that when the gap was insufficient, the expiring electrons did not gain enough energy to create defects in the structure of the crystal under study.

A high voltage of the order of 4-5 kV was created using a high-voltage rectifier. In this case, the difference from the one described earlier (see [5-7]) is the use of constant voltage for processing.

For processing in a gas discharge, samples were selected that had symmetrical linear CVC graphs both in the dark and in the light. Sufficiently photosensitive crystals were used. In both cases – both in the dark and under illumination – after the technological process, the total resistance of the crystal increased. After the appearance of electronic traps, the initially low-resistance area of the spatial charge of the ohmic contact significantly increases its resistance as a result of the formation of a barrier. The resistance of the base in the dark was ” $5 \prec 10^4$ Om, in the light $(2$–$3)10^4$ Om. A slight difference in the obtained values allows us to conclude that the width of the formed barrier is determined only by the depth of penetration of traps. There are very few traps in the layers far from the crystal surface, and therefore all of them are already filled in the dark. The light does not change their filling and, therefore, the width of the ASC, and with it the resistance.

When illuminated by strongly absorbed light, carriers are created in the near-surface layers of the sensor and are forced to move along the surface by the applied field. Gas discharge treatment promotes, according to [5,6], the formation of additional donor centers on the surface. At the same time, the surface conductivity increases, and the effect of recombination weakens.

8.7. Photoelectric properties of the obtained samples

In the spectral range 540–600 nm for samples pretreated in a gas discharge, we observed a slight increase in photocurrent. This indicates the predicted appearance of deep trap levels as a result of crystal processing.

The conditions for the formation of a barrier in our structures are also manifested in the dependence of the shape of the spectral distribution curve of the photocurrent on the polarity of the applied voltage. For conventional barriers, as the applied forward displacement increases, the height of the barrier and its width decrease. At the same time, the field strength in the ASC of the barrier, as the ratio of these values, changes little. When the polarity of the applied field is reversed, both these parameters – height and width – simultaneously increase, but their ratio again does not undergo significant changes.

In our case, this is not the case. The width of the formed barrier is determined only by the depth of penetration of traps and does not depend on the applied voltage. In this case, the external electric field lowers the height of the barrier and distorts its symmetry (see Figure 8.1). The side of the potential barrier in which the field strength is opposite to the external one decreases to a greater extent. Since one-way illumination is produced at the same time, the short-wave and long-wave part of the spec-

tral distribution curve of the photocurrent with a change in the polarity of the offset are distorted in different ways.

If, under the action of the applied field, the increasing – from the lighting side – half of the barrier is modified more (see Figure 8.1), then the short-wave (with strong light absorption) part of the spectral dependence changes significantly.

On the contrary, if the direction of the field is such that it mainly changes the back, falling side of the barrier, then basically changes should be expected for photocurrents excited by long-wave, deeply penetrating light.

Experimentally, it turned out to be more correct to investigate the spectral distribution of the emerging photo-EMF. This approach makes it possible not to take into account the nuances of photocurrent formation – recombination in the inner regions of the crystal, the influence of the resistances of its parts, etc. And instead, the main thing to identify is the influence of emerging traps in the near-surface layers of the sample due to processing in a gas discharge and donor levels on its geometric surface.

Without the participation of an external field on samples treated in a gas discharge, for longitudinal conductivity, we observed the occurrence and unusual distribution of EMF when excited by light of different wavelengths. The curve is shown in Figure 8.3.

In our case, we found that the value of the photo-EMF in white light up to 100 lk it turned out to be smaller than with monochromatic lighting. This is due to the unusual appearance of the graph Fig. 8.3. The short-wave and long-wave contributions do not add up, as usual, in white light, but are subtracted.

This happens because of the non-trivial type of barrier. As a rule, the ASC is represented either by an increasing part from the surface deep into the crystal (ohmic contact), or by a falling part (shut-off contact). In our case, both slopes of the barrier are represented (Fig. 8.1). It is all displaced in the volume of the crystal from the surface. In this regard, when illuminated from the contact side on the sample surface, absorption first occurs in the increasing part of the barrier for short wavelengths of light with strong absorption .

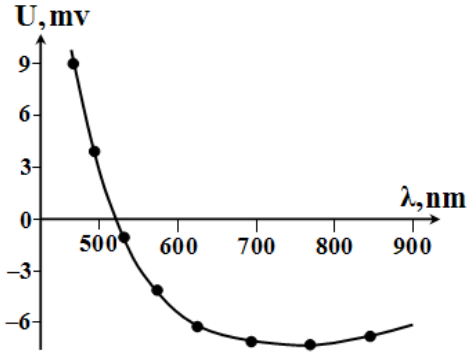

Fig. 8.3. Spectral distribution of photo-EMF. For crystals treated in a gas discharge

Photoexcited electrons by the barrier field return to the contact on the illuminated surface, where they increase the negative potential relative to the lower contact to the sample. In Figure 8.3, we took this value for the positive part of the curve (the area of 440-540 nm).

As can be seen from the figure, as the excitation wavelength increases, the contribution of this component decreases. This happens because the light absorption coefficient decreases for longer wavelengths, and some of the photons reach deeper layers of the crystal, where the falling part of the barrier is located. In this case, the field strength causes the nonequilibrium electrons to move in the opposite direction. Obviously, for a wavelength of 540 nm, when Fig. 8.3 there is an intersection of the graph and the abscissa axis, both of these processes balance each other and the resulting potential difference turns out to be zero.

With a further increase in the wavelength, more and more photons are absorbed from the side of the declining part of the barrier (Fig. 8.1). The barrier field mainly directs electrons deep into the sample, the negative potential of the lower contact increases.

At sufficiently large wavelengths of ~800 nm or more, the signal stabilizes (Fig. 8.3), remaining negative. This indicates the predominant absorption of light in the right side of the barrier (Fig. 8.1). In addition, part of the photons can penetrate deep enough into the crystal and be absorbed outside the contact ASC zone, without making any contribution to the formation of the graph Fig. 8.3.

The technological techniques used cause changes in this graph with a certain ratio of temperature, lighting, the intensity of the field used and the duration of processing. In our case, we got the best results when 15 min pro-

cessing with a distance of 8 mm to the needle on which it was 4000 V. Then the graph takes on an anomalous appearance with the largest possible area of negative values.

The limit of changes in the curve of Figure 8.3 is the usual spectral distribution of the photoresponse. If there is too much saturation of traps during processing in a gas discharge, the gradient of their concentration turns out to be insignificant, and the spectral distribution returns to its initial state. This is the same crystal in which the resistance has simply increased due to the presence of traps.

Thus, the proposed technology for creating sensors, in full accordance with the developed model, makes it possible to obtain sensors with abnormal spectral sensitivity. The type of dependence of Fig. 8.3 makes it possible to use them as receptors for a certain wavelength of radiation, predetermined in advance during processing. Moreover, since the signal value is zero at this point, such a sensor will be completely insensitive to any noise and interference, including artificially supplied.

In addition, when illuminated from different regions of the spectrum, the EMF sign, and hence the current, changes to the opposite. This property can be used to create a new generation of optical devices.

References

1. Simanovych N.S., Brytavskyi Ye.V., Kutalova M.I., Borshchak V.A., Karakis Y.N. “The study of heterogeneous sensitized crystals of cadmium sulfide. Part I. About charge state of the centers recombination” // “Photoelectronics”, n. 26. Odesa, 2017. P. 124 – 138 .
2. S.S.Kulikov, Ye.V. Brytavskyi, M.I., Kutalova, N.P. Zatovskaya, V.A. Borshchak, N.V. Konopel’skaya, Y.N. Karakis “The study of cadmium sulfide heterogeneously sensitized crystals. Part II. Relaxation characteristics” // “Photoelectronics”, №. 27. Odesa, 2018. P. 79 – 93 .
3. Kulikov S.S., Brytavskyi Ye.V., Kutalova M.I., Zatovskaya N.P., Borshchak V.A., Karakis Y.N. “The study of cadmium sulfide heterogeneously sensitized crystals. Part III. Oscillations of excited carriers”, // “Photoelectronics”, №. 28. Odesa, 2019. P. 133 – 144.
4. Kulikov S.S., Brytavskyi Ye.V., Kutalova M.I., Zatovskaya N.P., Borshchak V.A., Karakis Y.N. “The study of cadmium sulfide heterogeneously sensitized crystals. Part IV. Oscillations of excited carriers”, // “Photoelectronics”, №. 29. Odesa, 2019. P. 21-37.
5. Чемересюк Г.Г., Сердюк В.В. Явления, обусловленные захватом носителей, инжектированных в освещенные монокристаллы селенида кадмия // Известия высших учебных заведений. Физика.– 1968.– №12.– С.7 – 12.
6. Чемересюк Г.Г. Отрицательная фотопроводимость в селениде кадмия, обусловленная уменьшением подвижности свободных носителей // Studia Universitatis babes-bolyai: Series Physica Fasciculus 1.–1972. С. 21.
7. Чемересюк Г.Г., Сердюк В.В. Коротковолновое гашение продольной фотопроводимости монокристаллов селенида кадмия // Физика и техника полупроводников.-1969.-Т.3, в.3. С. 396-399.
8. Физика и химия соединений $A_{II}B_{VI}$.// Под ред. проф. С.А. Медведева.- М.: Мир, 1970. С. 103 – 104.
9. Драгоев А.А., Каракис Ю.Н., Балабан А.П., Чемересюк Г.Г. Расчёт профиля ОПЗ датчиков со знакопеременной спектральной чувствительностью // 4nd International Scientific and Technical Conference “Sensors Electronics and Microsystems Technology” SEMST-4). Україна, Одеса, 28 червня – 2 липня 2010 р. “Астропринт”. 2010. С. 192.
10. A.A. Dragoev, A.V. Muntjanu, Yu. N. Karakis, M. I. Kutalova Calculation for migration-dependent changes in near-contact space-charge regions of sensitized crystals // “Photoelectronics”, №. 19. Odesa “Astroprint” 2010. P. 74 – 78.
11. Минаева О.П. Влияние газового разряда на формирование энергетического барьера в приповерхностной области кристаллов сульфида кадмия // Материалы 63-й отчетной студенческой научной конференции. Секция физики полупроводников и диэлектриков.– Одесса, 2007, С. 3 – 4.

UDC621.315.592

Kulikov S.S., Brytavskyi Ye.V., Borshchak V.A., Zatovskaya N.P.,
Kutalova M.I., Karakis Y.N.

THE STUDY OF HOMOGENEOUS AND HETEROGENEOUS SENSITIZED CRYSTALS OF CADMIUM SULFIDE. PART V. INHOMOGENEOUS ALLOYING

Summary

The technology of CdS semiconductor crystals processing in the corona discharge is developed. It is established that as a result of this exposure, the samples acquire alternating spectral sensitivity. The observed phenomenon is explained by the emergence of a saddle of the potential barrier in the surface region of the element, the unusual properties which can allow the creation of a new type of device.

Keywords: inhomogeneous alloying, corona discharge, barrier structure

УДК 621.315.592

Куликов СС., Бритавский Е.В., Борщак В.А., Затовская Н.П.,
Куталова М.И., Каракис Ю.Н.

ИССЛЕДОВАНИЕ ОДНОРОДНЫХ И ГЕТЕРОГЕННЫХ СЕНСИБИЛИЗИРОВАННЫХ КРИСТАЛЛОВ СУЛЬФИДА КАДМИЯ. ЧАСТЬ V. НЕОДНОРОДНОЕ ЛЕГИРОВАНИЕ

Резюме.

Разработана технология обработки кристаллов полупроводников CdS в коронном разряде. Установлено, что в результате такого воздействия образцы приобретают переменную спектральную чувствительность. Наблюдаемое явление объясняется появлением седла потенциального барьера в приповерхностной области элемента, необычные свойства которого могут позволить создать новый тип устройства.

Ключевые слова: неоднородное легирование, коронный разряд, структура барьера

УДК 621.315.592

Куликов С.С., Бритавський Є.В., Борщак В.А., Затовська Н.П.,
Куталова М.І., Каракіс Ю.М.

ДОСЛІДЖЕННЯ ОДНОРІДНИХ І ГЕТЕРОГЕННИХ СЕНСИБІЛІЗОВАНИХ КРИСТАЛІВ СУЛЬФІДУ КАДМІЮ. ЧАСТИНА V. НЕОДНОРІДНЕ ЛЕГУВАННЯ

Реферат.

Розроблено технологію обробки кристалів напівпровідників CdS у коронному розряді. Встановлено, що в результаті такого впливу зразки набувають змінної спектральної чутливості.Спостережуване явище пояснюється появою сідла потенційного бар'єру в приповерхневій області елемента, незвичайні властивості якого можуть створити новий тип пристрою.

Ключові слова: неоднорідне легування, короний разряд, структура бар’єра.

This article has been received in October 22, 2021